



## Comparison of an Efficient Optimal Energy Management Strategy with a Rule-based One in Hybrid Electric Vehicles

Bentolhoda Eivani<sup>1</sup>, Hossein Moeinkhah<sup>2\*</sup>, Saeed Farahat<sup>3</sup>

<sup>1</sup>PhD Candidate in Department of Mechanical Engineering, University of Sistan and Baluchestan, Zahedan

<sup>2</sup>Professor, Department of Mechanical Engineering, University of Sistan and Baluchestan, Zahedan

<sup>3</sup>Professor, Department of Mechanical Engineering, University of Sistan and Baluchestan, Zahedan

ARTICLE INFO	ABSTRACT
<p><b>Article history:</b></p> <p>Received : 6 Jun 2024</p> <p>Accepted: 15 Sep 2024</p> <p>Published: 7 Oct 2024</p>	<p>This paper introduces a dynamic programming approach designed to address the challenge of optimal energy management in hybrid electric vehicle (HEV) powertrains and evaluates its effectiveness compared to a rule-based approach. Dynamic programming, as a trajectory-based optimization method, It provides a globally optimal solution and serves as a benchmark in support of evaluating other control strategies. Nonetheless, this method is significantly hampered by its high computational demands, often known as the curse of dimensionality, where the computation time and memory requirements increase exponentially as the number of states and inputs expands. The paper presents a novel strategy to mitigate this computational burden and demonstrates how this enhancement can lead to more precise outcomes.</p>
<p><b>Keywords:</b></p> <p>dynamic programming</p> <p>power split device</p> <p>HEV</p> <p>optimal energy management</p>	

### 1. Introduction

It is well-established hybrid electric vehicles (HEVs) possess the capability to greatly reduce fuel usage and the emission of greenhouse gases. Nevertheless, the ultimate performance and efficiency of an HEV largely depend on factors such as the choice of configuration, component sizing, and the design of the supervisory energy management strategy. HEVs typically come in three configurations: series, parallel, and series-parallel (or power-split). The series-parallel configuration is particularly notable because it brings together the benefits of both series and parallel configurations types while mitigating their respective drawbacks. Most modern HEVs

use power-split transmissions, which offer greater flexibility and a wider range of operational modes.

The the energy management approach is crucial for distributing power distribution among the powertrain components according to the vehicle's requirements. There are two main types of energy management approaches: rule-based methods and optimization approaches. Rule-based methods rely on heuristics, insight, and expert knowledge, and are predominantly used in real-time scenarios. These strategies can be divided further into deterministic methods and fuzzy rule-based approaches. In contrast, optimization methods

\*Corresponding Author  
Email Address: [hmoein@gmail.com](mailto:hmoein@gmail.com)  
<https://doi.org/10.22068/ase.2024.677>

involve minimizing a cost function through analytical or numerical processes to enhance powertrain efficiency and reduce losses. These are able to be categorized into global optimization strategies and real-time optimization approaches

Global optimization approaches evaluate the full driving cycle in advance to minimize the cost function, and are often used as benchmarks for comparing different energy management strategies. Dynamic programming is a prominent global optimization technique. Real-time optimization methods focus on minimizing instantaneous costs. The Equivalent Consumption Minimization Strategy (ECMS) is a widely recognized real-time approach [1-2].

Several studies have investigated the energy management of HEVs with power-split transmissions. He et al. [3] proposed an energy optimization strategy for power-split drivetrains in plug-in hybrid electric vehicles, utilizing predicted speed profiles and addressing real-time implementation issues such as optimization window sizes and the effects of Forecasting inaccuracies in energy estimation management strategy's performance. Wu et al. [4] introduced An advanced energy management approach for power-split systems plug-in hybrids at both trip and tour levels, incorporating prior Awareness of the vehicle's position, road conditions, and real-time traffic data to minimize fuel usage for the journey. This approach can additionally enhance energy efficiency at the tour stage if there is a pre-established travel schedule and information on battery recharging opportunities are available. Park et al. [5] enhanced the fuel efficiency of a power-split hybrid vehicle using the ECMS, which identifies The ideal allocation of power by transforming battery energy into equivalent fuel power while reducing total fuel consumption. They proposed a practical method to determine the ideal conversion factor using a direct search method and a vehicle simulation model. Chen et al. [6] developed A real-time and smart energy management controller for power-split plug-in hybrids, utilizing genetic algorithms and quadratic programming. In [7], A forward power-split plug-in hybrid model, integrated with an energy management system and cycle optimization algorithm, was assessed for its energy efficiency. Wang et al. [8] created a

suboptimal energy management strategy for the real-time management of a series-parallel hybrid electric bus, which was validated through a hardware-in-the-loop (HIL) simulation on PT-LABCAR. Johannesson et al. [10] proposed a predictive control scheme for a series-parallel hybrid bus, using GPS data and route information to optimize energy storage scheduling and mode switching. In [11], Li et al. developed a model predictive control (MPC) strategy to address the ideal energy management challenge in power-split hybrid vehicles. This approach involves linearizing the nonlinear powertrain model and constraints at each sampling time and utilizing a moving horizon linear approach MPC method. [12] used dynamic programming to optimize the planetary gear ratio in power-split plug-in hybrid vehicles.

This paper introduces a new approach for optimizing energy management in hybrid electric vehicles (HEVs) with power-split transmissions using dynamic programming. The goal is to achieve globally optimal performance while reducing computational load and improving accuracy by refining the state mesh density. The organization of the paper is as follows: Section 2 presents the mathematical model of the HEV; Section 3 reviews dynamic programming fundamentals, formulates the HEV's optimal control problem, and discusses methods to enhance computational efficiency; Section 4 compares the performance of this algorithm with the rule-based method from ADVISOR; and Section 5 concludes the paper.

## 2. Hybrid Electric Vehicle Model

The powertrain diagram of the hybrid electric vehicle (HEV) under study is depicted in Figure (1). This configuration, known as the Toyota Hybrid System (THS), is utilized in models such as the Prius and Camry hybrids [13]. In this setup, the primary components consist of the internal combustion engine, two electric motors (MG1 and MG2), a power split device (PSD), and the battery. The engine is linked to the carrier, while electric motor MG2 is attached to the ring gear and the final drive, functioning primarily as the electric motor. Electric motor MG1 is linked to the sun gear and mainly serves as a generator. The

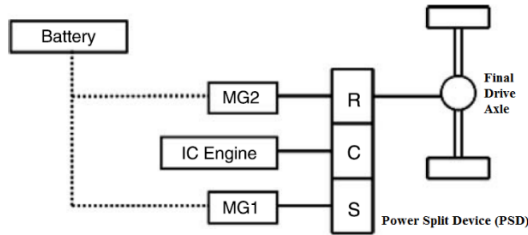


**Figure 1:** powertrain system of Toyota Prius (THS) [13]

battery accumulates energy generated by the electric motors during their generator operation or through energy recovery during regenerative braking.

## 2.1. Engine Model

For the supervisory control task, the focus is primarily on optimizing overall performance metrics such as power output, efficiency, and fuel consumption rather than delving into the intricacies of the process of combustion or high-frequency engine behavior. In this context, the engine's operational characteristics are abstracted using a look-up table, which simplifies the representation of fuel consumption based on engine velocity and the torque demands placed on the engine by the driver. This approach allows for a more streamlined analysis and control strategy, as the complex variables involved in the combustion process are effectively encapsulated in the table's data. By consulting the fuel consumption map, as illustrated in Figure (2), one can directly assess the relationship between engine speed and fuel consumption based on the torque requirements, facilitating more effective management of fuel efficiency and overall performance.

## 2.2. Motor/Generator Models

In the THS power split configuration, two electric machines are utilized, each able to functioning either as a motor or a generator. While both machines can contribute to vehicle

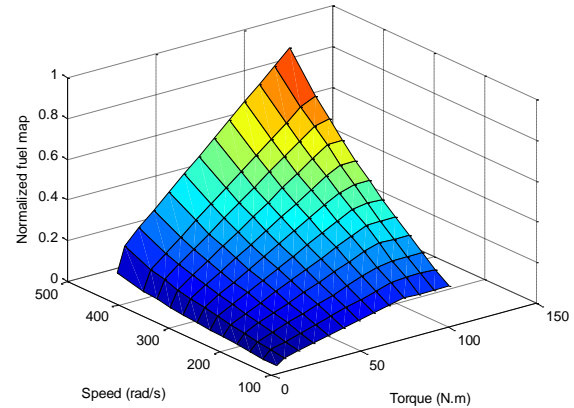


**Figure 2 :** THS engine look-up table

propulsion or resist its movement, MG2 primarily operates as a motor and MG1 as a generator. MG2, which is mounted on the same axle as the ring gear, is connected to the final drive via a torque-enhancing device to deliver driving force to the wheels. On the other hand, MG1, which is attached to the sun gear, manages engine speed adjustments and uses surplus power to charge the battery. Comprehensive parameters of the electric machines are presented in Table (1).

Table 1: Motor/Generator specifications [14]

Electric Machine	Parameter	Value
MG1	Max Power	±25 kW
	Max Torque	±55 N.m
MG2	Max Power	±40 kW
	Max Torque	±305 N.m

The mechanical power of an electric machine is determined as the product of torque and rotational speed. Therefore, the electric power can be expressed as:

$$P_{E-MG} = T_{MG} \omega_{MG} \eta^{-k} \quad (1)$$

Here,  $T_{MG}$  and  $\omega_{MG}$  represent the torque and rotational speed, respectively.  $\eta$  denotes the effectiveness coefficient, and  $k$  indicates the direction of the mechanical power. If the motor-

generator (MG) is consuming energy (positive power),  $k=-1$ , and if the MG is producing energy (negative power),  $k=1$  [15]. The efficiency of each electric machine is provided by a reference dataset, derived from the ADVISOR database [14].

## 2.3. Battery Pack Simulation Model

The battery module incorporated into this model is a 4.4 kW.hr Li-ion one with the specifications detailed in Table 2. To model the charge state (SOC) behavior of this battery pack, an equivalent circuit model for internal resistance is utilized. This approach ensures the necessary accuracy for SOC dynamics and is sufficiently suitable for integration into an optimization framework. The battery output power can be obtained as [16]:

$$P_b = VI - RI^2 \quad (2)$$

Where  $V$  represents the open circuit voltage of the battery pack and relies on the pack's state of charge (SOC),  $R$  is the internal resistance and is influenced by the SOC and the electric current flow (or  $I$ ) direction. The dynamics of the battery pack are influenced by the rate of change in SOC and can be expressed as [16]:

$$\dot{SOC} = \frac{-I}{Q_{pack}} \quad (3)$$

Where,  $Q_{pack}$  represents the highest storage capacity of the battery pack.. Combining equations (2) and (3) results the relationship between the battery SOC and power as:

$$\dot{SOC} = \frac{-V - \sqrt{V^2 - 4P_b R}}{2RQ_{pack}} \quad (4)$$

The power consumed or supplied by the battery pack through the electric machines can be calculated as:

$$P_B = P_{E-MG1} + P_{E-MG2} \quad (5)$$

**Table 2:** Battery parameters [14]

Parameter	Value
Storage capacity	7.035 A.hr
Nominal Voltage	633 V
Max Discharge Power	40 kW
Max Charge Power	35 kW

## 2.4. Power Split Device Model

As shown in Figure (3), the power split device includes a carrier, a ring gear, and a sun gear and some planets. The carrier gear is linked to the engine, while the ring gear is linked to both MG2 and the output axle, the sun gear is attached to MG1, and the planet gears are responsible for transferring force between the different gears. The following kinematic relationship holds among the gears [13]:

$$\omega_r R + \omega_s S = \omega_c (R + S) \quad (6)$$

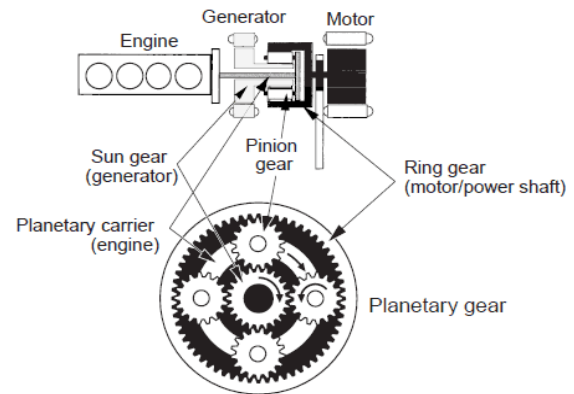


**Figure 3:** power split device [16]

Where  $R$  and  $S$  denote The tooth count on the ring and sun gears, in that order, and represent the rotational speeds of the ring gear, sun and carrier gears, respectively. The illustrated PSD is an input-splitting device during regular operation where the carrier gear serves as the input gear and the ring and sun gears function as the output gears. The relationships between the torques are as follows [13]:

$$T_s = -\frac{S}{R+S}T_c \quad (7)$$

$$T_R = -\frac{R}{R+S}T_c \quad (8)$$

Where  $T_c$ ,  $T_R$  and  $T_s$  are the torques applied on carrier, ring and sun gears, respectively.

## 2.5. Full Powertrain Model

Free body representation of the THS powertrain is illustrated in Figure (4). The rotational equations at the sun, carrier and ring gears are as follows:

$$\dot{\omega}_{MG1} I_{MG1} = F.S + T_{MG1} \quad (9)$$

$$\dot{\omega}_e I_e = T_e - F.R - F.S \quad (10)$$

$$\dot{\omega}_r (I_{MG2} + \frac{R_{tire}^2}{K^2} M) = T_{MG2} + F.R - T_{load} \quad (11)$$

Where,  $I_e$ ,  $I_{MG1}$  and  $I_{MG2}$  are the inertia of the engine, MG1 and MG2, respectively.  $R_{tire}$  is the tire radius,  $K$  represents the overall gear ratio, and  $F$  denotes the internal interaction force between the planet pinions and each gear.  $T_{load}$  is the resisting torque and is obtained as:

$$T_{load} = (0.5\rho C_D A_f v^2 + mg \sin \alpha + f_r mg \cos \alpha) R_{tire} + T_f \quad (12)$$

where the first term in parentheses represents aerodynamic drag friction, the second term represents resistance encountered while going uphill, and the third component indicates rolling drag.;  $T_f$  denotes the braking torque generated by the friction brake system.

## 3. Dynamic Programming Optimization

Dynamic programming is an approach that technique used for optimizing trajectories by determining a sequence of control actions that produce a state trajectory within a quantized domain, aiming to minimize a cumulative cost function. This approach ensures a globally optimal solution as long as certain constraints on states and inputs are satisfied. In this context, the

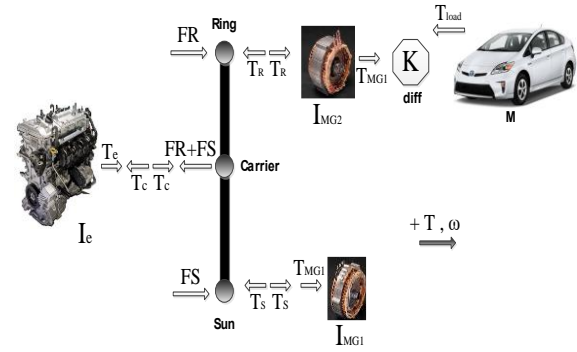


**Figure 3:** free body diagram of the THS powertrain

objective of dynamic programming is to determine the optimal series of control decisions at each time interval  $k$  that reduces the cost criterion [17]:

$$J = G_N(x(N)) + \sum_{k=1}^n L_k(x(k), u(k), w(k)) \quad (13)$$

For which

$$x(k+1) = f(x(k), u(k), w(k)) \quad (14)$$

Subject to

$$x(k) \in X(k) \quad u(k, x) \in U(k) \quad (15)$$

represents the immediate transition cost,  $G_N$  is the endpoint cost at  $k=N$ .  $x(k)$  is the state vector in the state space  $X(k)$ ,  $u(k)$  is the vector of control inputs within the input space  $U(x(k), k)$ ,  $w(k)$  is known interference and  $f$  depicts the system motion.

The issue can be stated with limitations on the state and input Parameters:

$$g_i(x(k)) \leq 0 \quad i = 1, 2, \dots, q \quad (16)$$

$$h_i(u(k)) \leq 0 \quad i = 1, 2, \dots, p \quad (17)$$

Bellman's rule of Optimality is applied to solve the formulated optimization challenge [18].

### 3.1. Application of Dynamic Programming to the HEV

The initial stage in implementing dynamic programming to the power management issue of hybrid electric vehicles (HEVs) is to identify the states and control inputs that need to be discretized. The full set of system situations and inputs discussed in the previous section are listed in Table (3).

**Table 3:** system total states and inputs

States	Inputs
$\omega_e$ : engine rotational speed	$T_e$ : engine torque
$\omega_r$ : ring gear rotational speed	$T_{MG1}$ : MG1 torque
$\omega_s$ : sun gear rotational speed	$T_{MG2}$ : MG2 torque
$SOC$ : state of charge	$off/on$ : decision of engine being off or on

Given that the behavior of the battery's State of Charge (SOC) are independent of the mechanical situations and directly influence the control decisions for power allocation between the internal combustion engine and the battery module at any given moment, it is necessary to discretize the SOC. Likewise, since determining the engine's operational status (whether it is on or off) at any given time is essential, the engine speed must also be discretized.

The power-splitting control policy is essential for hybrid vehicle performance, as it manages the allocation of power between the internal combustion engine and the battery pack to meet the vehicle's dynamic power demands. It optimizes fuel consumption and maintains battery charge by balancing power between the two sources based on factors like speed and load. This system reduces fuel use in low-demand situations by favoring electric power and relies more on the engine during high-demand scenarios. Overall, this efficient power management enhances vehicle performance, reduces engine wear, and extends battery life.. When the engine torque is meshed and, considering that the engine speed is also meshed,

the engine's power contribution is established. This approach eliminates the need to mesh the torque of MG1, a method used in previous studies [19, 20]. By adopting this new logic, one less input needs meshing, which significantly reduces the required computation time and memory. Since the driving cycle is predetermined in this optimization technique, the velocity and rate of change of velocity of the ring gear can be calculated in the role of proceeds:

$$\omega_r = \frac{K}{R_{tire}} v \quad \text{and} \quad \dot{\omega}_r = \frac{K}{R_{tire}} \dot{v} \quad (18)$$

Considering that  $\omega_r$  is known and  $\omega_e$  is meshed,  $\omega_s$  can be obtained by using equation (6). By knowing  $v$  and  $\dot{v}$ , the power demand at each time step can be calculated as:

$$P_{dem} = F_{drive} v \quad (19)$$

The connection between the power demand and the overall output power of the powertrain can be expressed as:

$$P_{dem} = T_e \omega_e + T_{MG1} \omega_s + T_{MG2} \omega_r \quad (20)$$

Now, all the equations can be solved for any unknown parameter considering engine ON or OFF operation (Table 4).

**Table 4:** system description in every engine operation mode

Engine Mode	Description
OFF	<ul style="list-style-type: none"> <li>The carrier gear is locked to the ground (<math>\omega_e=0</math>).</li> <li><math>\omega_r</math> and <math>\dot{\omega}_r</math> are known from the driving cycle.</li> <li><math>\omega_s</math> and <math>\dot{\omega}_s</math> are obtained from the kinematic constraint.</li> <li>Using equations (9), (11) and (20), <math>F</math> can be calculated. If vehicle is not moving <math>F=0</math>. Then the electric machines torques can be calculated.</li> </ul>

Engine Mode	Description
ON	<ul style="list-style-type: none"> <li>The carrier gear is free to rotate (<math>\omega_e \neq 0</math>).</li> <li>By combining equations (6), (9), (10), (11) and (20), <math>F</math>, <math>T_{MG1}</math>, <math>T_{MG2}</math>, <math>\dot{\omega}_s</math> and <math>\dot{\omega}_e</math> will be calculated.</li> </ul>
Start-up	<ul style="list-style-type: none"> <li>The carrier gear is free to rotate during transitions between engine ON and OFF modes. Hence the same dynamics for the engine ON mode is true here.</li> <li>Simplification in this mode:</li> </ul>
Shut-down	$\dot{\omega}_e = \frac{\omega_{rev}}{dt}$ for start-up and $\dot{\omega}_e = -\frac{\omega_e}{dt}$ for shut-down. <p>MG1 is responsible for reducing the engine speed to zero during shut-down or revving the engine up to an operable speed, <math>\dot{\omega}_{rev}</math>.</p> <ul style="list-style-type: none"> <li><math>\dot{\omega}_s</math> and <math>F</math> can be calculated by equations (6) and (10), respectively. Then, <math>T_{MG1}</math> and <math>T_{MG2}</math> can be obtained.</li> </ul>

Now, considering that  $\omega_e$  and  $SOC$  are meshed as states and  $Te$  and *off/on decision* are meshed as inputs, the optimization problem aims to reduce fuel consumption based on the following cost function:

$$J = \sum_{k=1}^n FC_k \quad (21)$$

Constraining by equation (14) where  $w(k)$  is the velocity profile obtained from the driving process. Limitation of the engine, the battery pack and the electric machines are stated in terms of some constraints to the states and inputs and any breach of a constraint results in the imposition of a significant penalty cost.

$$\omega_{e,min} \leq \omega_e \leq \omega_{e,max}$$

$$\omega_{s,min} \leq \omega_s \leq \omega_{s,max}$$

$$\omega_{r,min} \leq \omega_r \leq \omega_{r,max}$$

$$SOC_{min} \leq SOC \leq SOC_{max}$$

$$T_{e,min} \leq T_e \leq T_{e,max}$$

$$T_{MG1,min} \leq T_{MG1} \leq T_{MG1,max}$$

$$T_{MG2,min} \leq T_{MG2} \leq T_{MG2,max}$$

$$P_{e,min} \leq P_e \leq P_{e,max}$$

$$P_{MG1,min} \leq P_{MG1} \leq P_{MG1,max}$$

$$P_{MG2,min} \leq P_{MG2} \leq P_{MG2,max}$$

$$P_{batt,min} \leq P_{batt} \leq P_{batt,max}$$

(22)

In this study, the nearest neighbor approach is employed to achieve an accurate control policy [21]. When the meshing space is coarse, Significant gaps in between mesh points in the state and input grids not only lead to inaccuracies in the behavior but also result in the next state, calculated from a specific input, not necessarily aligning with a point on the state mesh. While linear interpolation could address this issue, it becomes challenging when limit constraints are applied to the state variables, in terms of the cost of violating these constraints can blend along with the actual transition cost. However, in the method proposed here, after calculating the next state based on a particular input, the state is adjusted to the nearest discrete point on the state grid. Although this approach requires finer meshing, which increases the computational load, it leads to more precise control policies.

#### 4. Optimization Performance

In this part, the efficiency of the proposed optimization method is evaluated against the rule-based strategy designed for energy management of the Toyota Prius HEV within the ADVISOR software. The comparison is conducted using the well-known Urban Dynamometer Driving Cycle (UDDS), which Models an urban route with



Comparison of an Efficient Optimal Energy Management Strategy with a Rule-based One in Hybrid Electric Vehicles

regular halts and includes two stages: the first 505 seconds make up the initial phase, and the remaining 876 seconds comprise the subsequent phase [22]. The specifications of this driving cycle are provided in Table 5. Diagrams showing velocity versus time and power demand versus time for this driving cycle are presented in Figure 5.

Table 5: driving cycles specifications [14]

Driving Cycle	Specifications
UDDS	Time= 1369 s
	Distance= 11.99 km
	Max speed= 91.25 km/h
	Average speed= 31.51 km/h
	Max acceleration=1.48 m/s <sup>2</sup>
	Average acceleration=0.5 m/s <sup>2</sup>
	Max acceleration=-1.48 m/s <sup>2</sup>
	Average acceleration=-0.58 m/s <sup>2</sup>
	Idle time=259 s
	No. of stops= 17
	Max up/down grade= 0%
	Average up/down grade= 0%

Table (6) illustrates the fuel usage of the HEV under the two distinct energy management strategies. As illustrated, the fuel consumption using the efficient global optimization strategy developed in this study is significantly lower than that of the rule-based method. The lower fuel consumption achieved by the dynamic programming algorithm is expected, given that it utilizes the driving cycle as a priori information. However, the substantial difference in results highlights the inadequacies in the design of the rule-based algorithm for the HEV within ADVISOR.

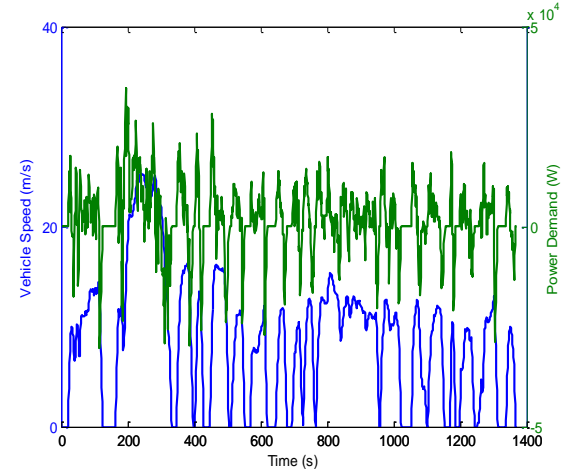


Figure 5: UDDS driving cycle

Table 6: Fuel consumption results

Energy Management Strategy	Fuel Consumption (grams)
Dynamic Programming	158
Rule-based method	406

Figures (6) through (8) depict the torques regarding internal combustion engines and electric machines for both strategies. As observed, the dynamic programming method results in the engine applying less torque compared to the rule-based method used in ADVISOR, which could contribute to reduced fuel consumption. However, the torque generated by MG2 under the dynamic programming algorithm is significantly higher throughout the cycle. This indicates that MG2 is the primary provider of the HEV's required power during the driving cycle, drawing its energy from the battery pack. In instances of significant charge depletion by MG2, MG1—powered by the engine—applies an appropriate amount of torque to help maintain the battery's SOC (Figure 9).

Rotational speeds of the components are presented in Figures 10 and 12. The speed of the ring gear remains consistent across both methods since it is linked to the wheels, which have their



speeds determined by the driving cycle. The engine speed resulting from dynamic programming is notably lower than that obtained through the rule-based method, potentially leading to greater fuel efficiency.

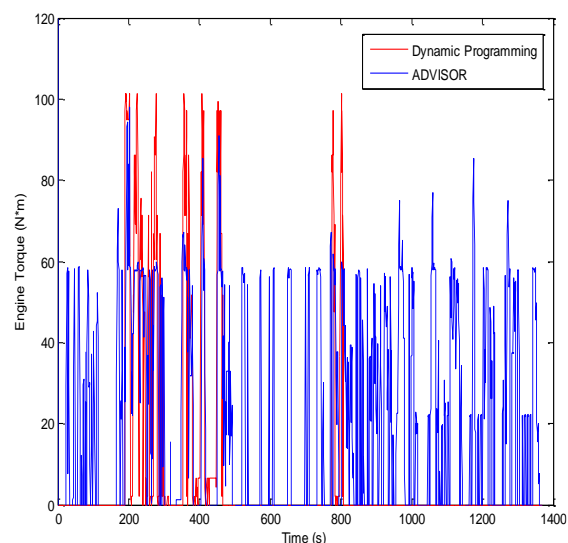


**Figure 6:** Engine torque

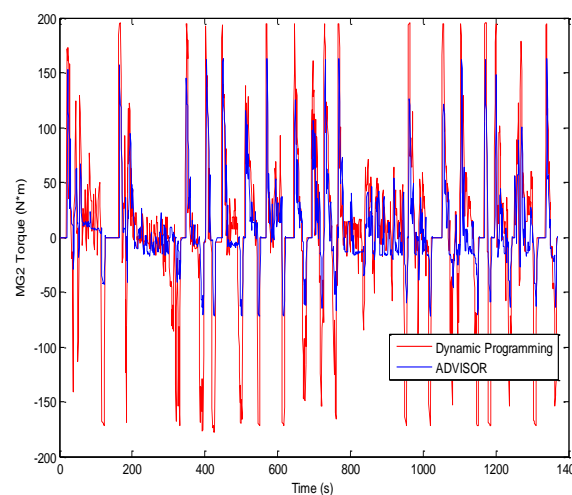


**Figure 7:** MG2 torque

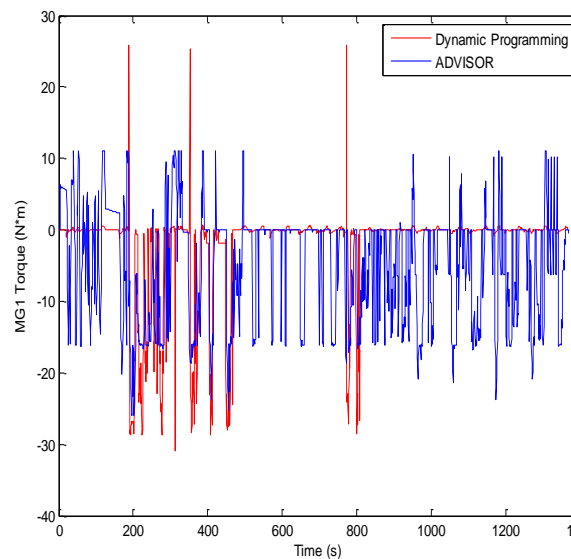


**Figure 8:** MG1 torque

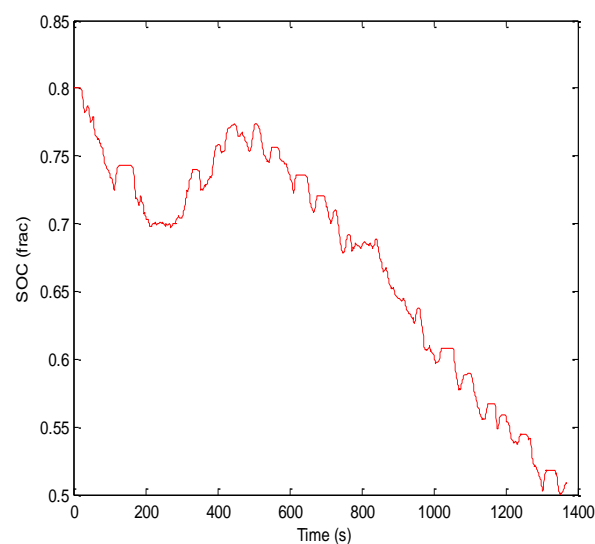


**Figure 9:** State of Charge (SOC) history

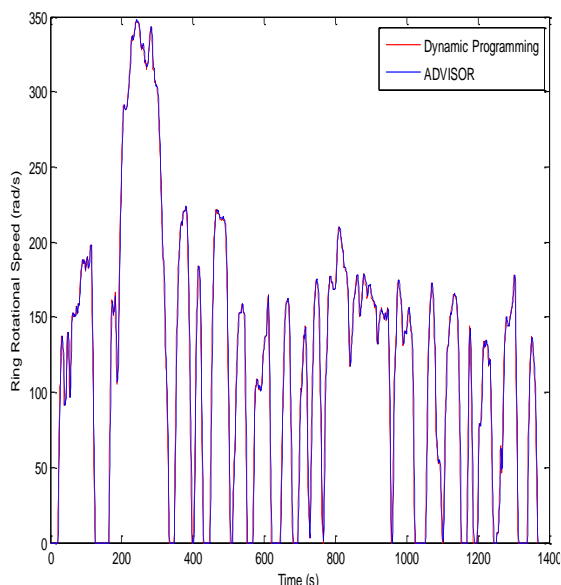


Figure 10: Rotational speed of the ring

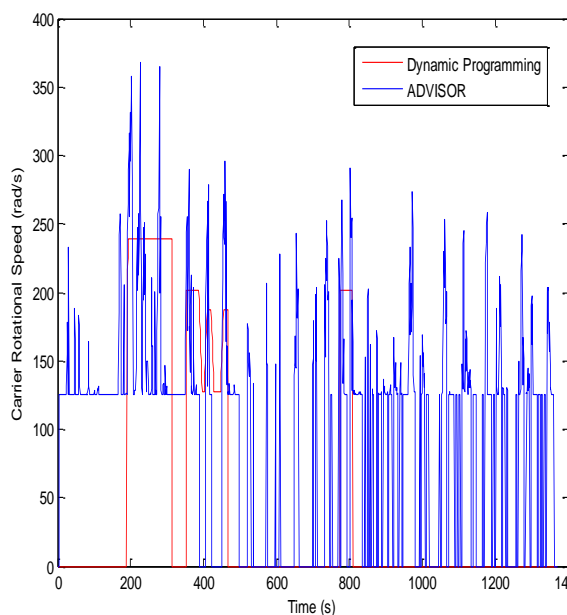


Figure 11: Rotational speed of the carrier

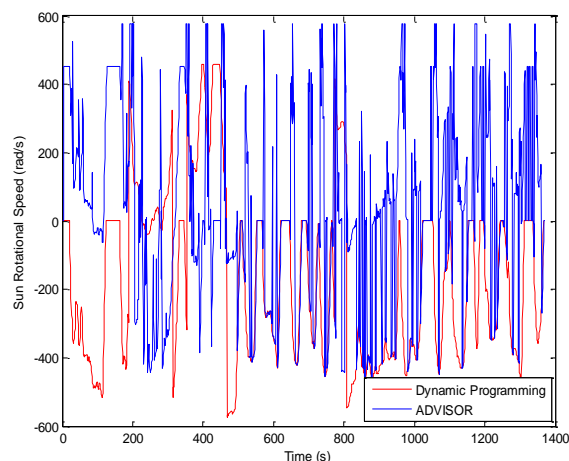


Figure 12: Rotational speed of the sun

## 5. Conclusion

In this paper, an innovative approach is implemented to develop a more efficient dynamic programming algorithm that reduces computational load while providing more accurate results. To achieve this, a comprehensive hybrid electric vehicle (HEV) model was introduced. Building upon this model and the principles of dynamic programming, the new method was designed by reducing the number of states and increasing mesh density. The effectiveness of this method was tested using the UDDS driving cycle and compared with the rule-based method from ADVISOR. The results demonstrated that this method is highly efficient, with significantly lower computational requirements, making it suitable for near real-time applications.

## References

- [1] K. Li and X. Zhang, "Optimal Control for Hybrid Electric Vehicles: A Review," *Energy Reports*, Vol. 6, pp. 239-258, 2020.
- [2] Y. Wang, J. Zhang, and Z. Wei, "Review of Optimization Techniques for Energy Management in Hybrid Electric Vehicles," *Journal of Power Sources*, Vol. 490, Article 229452, 2021.

- [3] H. He, Z. Zhang, and Y. Ding, "Energy Optimization Strategy for Power-Split Drivetrains in Plug-in Hybrid Electric Vehicles," *IEEE Transactions on Vehicular Technology*, Vol. 71, No. 8, pp. 8564-8575, 2022.
- [4] Z. Wu, H. Liu, and Q. Zhao, "Intelligent Energy Management Strategy for Power-Split Plug-in Hybrids Using Real-Time Data," *Transportation Research Part C: Emerging Technologies*, Vol. 147, Article 102178, 2023.
- [5] S. Park, H. Lee, and S. Kim, "Enhancing Fuel Economy of Power-Split Hybrid Vehicles with ECMS," *Energy Conversion and Management*, Vol. 244, Article 114493, 2022.
- [6] L. Chen, J. Wu, and J. Zhang, "Online Intelligent Energy Management for Power-Split Plug-in Hybrids Using Genetic Algorithms," *Control Engineering Practice*, Vol. 109, Article 104778, 2021.
- [7] Y. He, J. Rios, M. Chowdhury, P. Pisu, and P. Bhavsar, "Forward power-train energy management modeling for assessing benefits of integrating predictive traffic data into plug-in-hybrid electric vehicles," *Transportation Research Part D*, 2012, DOI: 10.1016/j.trd.2011.11.001.
- [8] M. Wang, Q. Li, and W. Liu, "Real-Time Energy Management Strategy for Series-Parallel Hybrid Electric Buses," *IEEE Transactions on Intelligent Transportation Systems*, Vol. 24, No. 5, pp. 6520-6532, 2023.
- [9] S. Dongye, L. Xinyou, Q. Datong, and D. Tao, "Power-balancing instantaneous optimization energy management for a novel series-parallel hybrid electric bus," *Chinese Journal of Mechanical Engineering*, 2012, DOI: 10.3901/CJME.2012.
- [10] J. Johansson, T. Bäckström, and T. Vanhatalo, "Predictive Control for Series-Parallel Hybrid Buses Using GPS and Route Information," *Automatica*, Vol. 136, Article 110092, 2022.
- [11] H. A. Borhan, A. Vahidi, A. M. Philips, M. L. Kuang, and I. V. Kolmanovsky, "MPC-based energy management of a power-split hybrid electric vehicle," *IEEE Transactions on Control Systems Technology*, Vol. 20, No. 3, 2012, DOI: 10.1109/TCST.2011.2134852.
- [12] C. Li, Y. Huang, and Y. Song, "Dynamic Programming for Planetary Gear Ratio Optimization in Power-Split Plug-in Hybrids," *Vehicle System Dynamics*, Vol. 61, No. 3, pp. 403-420, 2023.
- [13] B. Mashadi, "Vehicles Powertrain Systems", John Wiley & Sons, 2012.
- [14] Advanced Vehicle Simulator (ADVISOR 2003), <http://adv-vehicle-sim.sourceforge.net/>.
- [15] J. Liu, "Modeling, configuration and control optimization of power split hybrid vehicle", PhD thesis, University of Michigan, 2007.
- [16] Y. Li and N. C. Kar, "Advanced design approach of power split device of plug-in hybrid electric vehicles using dynamic programming", *Vehicle Power and Propulsion Conference (VPPC)*, IEEE, 2011.
- [16] <http://community.headlightmag.com/index.php?topic=43521.0>, accessed on 1 Dec 2015.
- [17] optimal control of hev book
- [18] R. E. Bellman, "Dynamic Programming", Princeton University Press, NJ, 1957.
- [19] J. Liu et al., "Modeling and Analysis of the Toyota Hybrid System", *Proceedings of the 2005 IEEE/ASME International Conference on Advanced Intelligent Mechatronics*, pp. 134-139, Monterey, CA, July 2005.
- [20] J. Liue and H. Peng, "Modeling and Control of a Power-Split Hybrid Vehicle", *IEEE Transaction on Control Systems Technology*, vol. 16, no. 6, pp. 1242-1251, Nov. 2008.
- [21] computationally efficient
- [22] Urban Dynamometer Driving Schedule, "https://en.wikipedia.org/wiki/FTP-75", accessed on 10 Dec 2015.